

Mesoporous In₂O₃ nanocrystals: synthesis, characterization and NO_x gas sensor at room temperature

Jun Gao^{‡a}, Hongyuan Wu^{‡a,c}, Jiao Zhou^a, Liyuan Yao^a, Guo Zhang^a, Shuang Xu^a, Yu Xie^d, Li Li^{*a},
^b, Keying Shi^{*a}

^a Key Laboratory of Functional Inorganic Material Chemistry, Ministry of Education. Key Laboratory of Physical Chemistry, School of Chemistry and Material Science, Heilongjiang University, Harbin, 150080, P. R. China.

^b Key Laboratory of Chemical Engineering Process & Technology for High-efficiency Conversion, School of Chemistry and Material Science, Heilongjiang University, Harbin 150080, P. R. China.

^c College of Chemistry and Chemical Engineering, Qiqihar University, Qiqihar 161006, P.R. China

^d Department of Materials Chemistry, Nanchang Hangkong University, Nanchang 330063, P.R. China

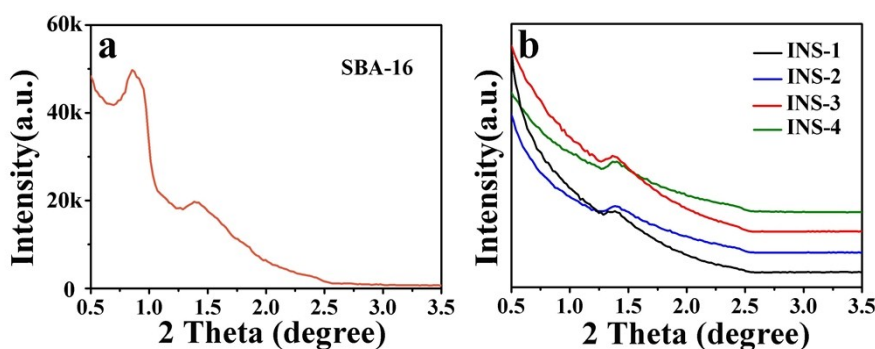


Fig. S1 Low-angle XRD X-ray diffraction diagrams of SBA-16 (1) and mesoporous In₂O₃ materials replicated from mesoporous silica of INS-1, INS-2, INS-3, INS-4. respectively.

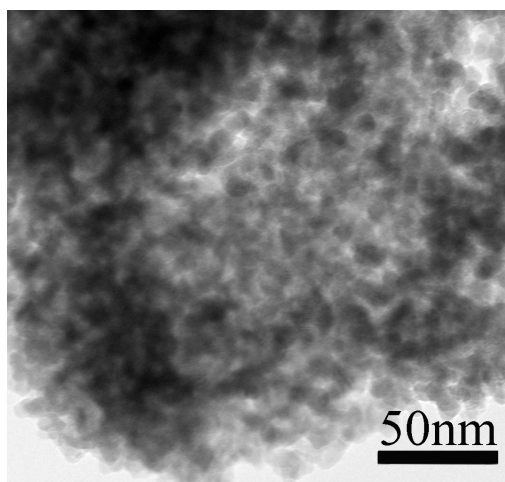


Fig. S2 TEM image of the INS-2.

Fig.S2 exhibited INS-2 sample was composed of In_2O_3 nanoparticles (5~10 nm) with some mesopores.

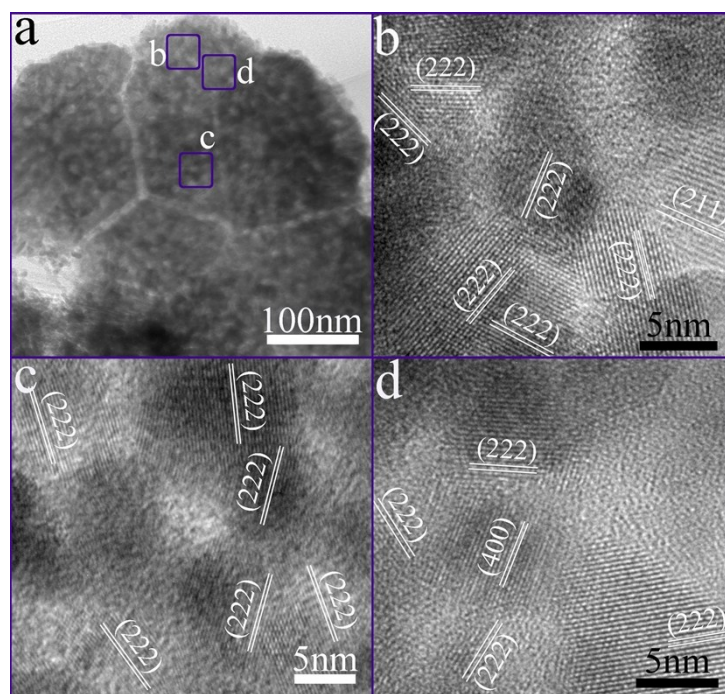


Fig. S3 TEM/HRTEM images of the INS-3. (a) TEM image, (b-d) HRTEM images of (a) INS-3.

Table S1 Comparison of the response-recovery results of response and response time(s) with different samples to NO_x (RH: 42%)

| Volume concentration /ppm | | 97.0 | 48.5 | 29.1 | 9.70 | 4.85 | 2.91 | 0.97 |
|---------------------------|-----------------|-------|------|------|------|------|------|------|
| INS-1 | Response | 9.74 | 3.81 | 3.42 | 2.7 | 0.53 | - | - |
| | Response time/s | 105 | 131 | 56 | 167 | 35 | - | - |
| INS-2 | Response | 41.2 | 17.7 | 13.5 | 5.36 | 1.58 | 1.19 | 1.2 |
| | Response time/s | 196 | 276 | 409 | 450 | 409 | 323 | 165 |
| INS-3 | Response | 158.7 | 50.7 | 36.8 | 19.7 | 12.6 | 7.2 | 1.9 |
| | Response time/s | 87 | 65 | 206 | 131 | 48 | 49 | 45 |
| INS-4 | Response | 7.39 | 6.9 | 5.84 | 4.4 | 0.76 | - | - |
| | Response time/s | 267 | 200 | 257 | 333 | 89.3 | - | - |

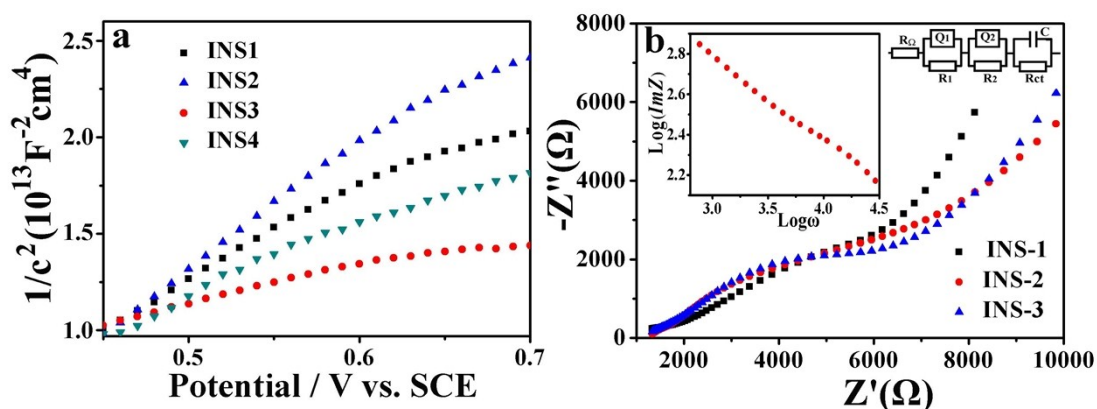


Fig. S4 (a) The Mott-Schottky curves of INS-1, INS-2, INS-3 and INS-4 samples, (b) The EIS curves of INS-1, INS-2 and INS-3 samples. The right inset is the corresponding equivalent circuit model, the inset in left shows the logarithmic plot of the imaginary part of the impedance.

Here R_{Ω} indicates the uncompensated bulk resistance of the electrolyte, separator and electrode. The Q1R1 parallel element corresponds to the electrode film interface capacitance (Q1) and the surface pore resistance (R1).¹ The Q2R2 parallel element might be attributed to the possible break

down of the electrolyte and the electrode material's internal microstructures. R_{ct} is attributed to the charge-transfer resistance at the active material interface and C is the constant phase angle element, involving double layer capacitance.

Table S2 Carrier concentrations and fitted impedance parameters of the INS-1, INS-2 and INS-3.

| Samples | $R_{\Omega}(\Omega)$ | $R_1(\Omega)$ | $R_2(\Omega)$ | $R_{ct}(\Omega)$ | Carrier concentration (cm^{-3}) |
|---------|----------------------|--------------------|---------------|--------------------|---|
| INS-1 | 972.8 | 5.71×10^5 | 1987 | 5.67×10^4 | 3.7×10^{17} |
| INS-2 | 846.6 | 3.34×10^5 | 2509 | 4.89×10^4 | 2.7×10^{17} |
| INS-3 | 562.4 | 6639 | 1314 | 125.2 | 9.3×10^{17} |

Notes and references

- 1 R. Sakamoto, Sh. Katagiri, H. Maeda, H. Nishihara, *Coordination Chemistry Reviews*, 2013, **257**, 1493-1506.